Tail-propelled aquatic locomotion in a theropod dinosaur

Authors: Nizar Ibrahim*[1], Simone Maganuco[2,3], Cristiano Dal Sasso[4], Matteo Fabbri[5], Marco Auditore[6], Gabriele Bindellini[7,6], David M. Martill[8], Samir Zouhri[9], Diego Mattarelli[6], David M. Unwin[10], Jasmina Wiemann[5], Davide Bonadonna[3], Ayoub Amane[9], Juliana Jakubczak[1], Ulrich Joger[11], George V. Lauder[12], Stephanie E. Pierce*[12]

Affiliations:

[1]Department of Biology, University of Detroit Mercy, Detroit, MI 48221, USA.

[2] Associazione Paleontologica Paleoartistica Italiana, 43121 Parma, Italy.

[3] Associate of 4.

[4] Sezione di Paleontologia dei Vertebrati, Museo di Storia Naturale di Milano, 20121 Milan, Italy.

[5] Department of Geology & Geophysics, Yale University, New Haven, CT 06511, USA.

[6] Collaborator of 4.

[7] Dipartimento di Scienze della Terra "A. Desio", Università degli Studi di Milano, 20133 Milan, Italy.

[8]School of the Environment, Geography and Geological Sciences, University of Portsmouth, Portsmouth, PO1 3QL, UK.

[9]Department of Geology, Faculty of Sciences Aïn Chock, Hassan II University of Casablanca, Morocco.

[10]School of Museum Studies, University of Leicester, Leicester LE1 7RF, United Kingdom

[11]Staatlich Naturhistorisches Museum Braunschweig, 38106 Braunschweig, Germany.

[12]Museum of Comparative Zoology and Department of Organismic and Evolutionary Biology, Harvard University, Cambridge, MA 02138, USA.

*Correspondence to: ibrahini@udmercy.edu and spierce@oeb.harbard.edu

Intensive research on non-avian dinosaurs in recent decades strongly suggests that they were restricted to terrestrial environments[1]. Historical views proposing that some groups, such as sauropods and hadrosaurs, lived in aquatic environments[2,3] were abandoned decades ago[4,5,6]. Recently, however, it has been argued that at least some spinosaurs, an unusual group of large-bodied Cretaceous theropods, were semi-aquatic[7,8], but this idea has been challenged on anatomical, biomechanical, and taphonomic grounds and remains controversial[9,10,11]. Here we present the first unambiguous evidence for an aquatic propulsive structure in a dinosaur, the giant theropod *Spinosaurus aegyptiacus*[7, 12]. This dinosaur has a tail with an unexpected and unique shape consisting of extremely tall neural spines and elongate chevrons forming a large, flexible, fin-like organ capable of extensive lateral excursion. Using a robotic flapping apparatus to measure undulatory forces in physical tail models, we show that the tail shape of *Spinosaurus* produces greater thrust and efficiency in water than the tail shapes of terrestrial dinosaurs, comparable to that of extant aquatic vertebrates that use vertically expanded tails to generate forward propulsion while swimming. This conclusion is consistent with a suite of adaptations for an aquatic lifestyle and a piscivorous diet in *Spinosaurus*[7,13,14]. Although developed to a lesser degree, similar aquatic adaptations are found in other spinosaurids[15,16] – a clade with a near global distribution and a stratigraphic range of more than 30 million years[14] documenting a persistent and significant invasion of aquatic environments by dinosaurs.

Detailed anatomical and functional studies, combined with abundant trackways, all point to a strictly terrestrial ecology for dinosaurs[1] with one clade, Maniraptora, taking to the air[17]. Dinosaurs are not currently thought to have invaded aquatic environments following the abandonment, several decades ago[5,6], of century old ideas of semi-aquatic habits in sauropods and hadrosaurs[2,3]. Recently, potential semi-aquatic lifestyles have been hypothesised for a small number of dinosaurs[18,19]. However, the only group of dinosaurs for which multiple plausible lines of evidence indicate aquatic adaptations are the spinosaurids, large-bodied theropods interpreted as near shore waders that fed on fish along the margins of, rather than within, water bodies[15,20,10].

A recent reappraisal of the largest known spinosaurid, *Spinosaurus aegyptiacus*, identified a series of adaptations consistent with a semi-aquatic lifestyle, including reduced hindlimbs, wide feet with large, flat unguals, long bones with a highly reduced medullary cavity, and a suite of cranial features such as retracted nares, interlocking conical teeth and a sensory rostromandibular integumentary system[7]. This interpretation has been challenged on the basis of taphonomy[8], biomechanical modeling[10], and anatomical concerns[8]. Locomotion in water is a major point of contention[10,11], because no unambiguous evidence for a plausible mode of propulsion has been presented. Furthermore, our understanding of the anatomy and ecology of this highly derived theropod has been hampered by the fact that only one associated *Spinosaurus* skeleton exists, with all other associated remains having been destroyed in World War II[7]. The posterior portion of the skeleton, in particular the caudal vertebral series, which has the potential to shed light on likely adaptations for aquatic locomotion, has, until recently, been poorly understood[12]. Consequently, the tail anatomy and function of *Spinosaurus* has been reconstructed on the basis of highly incomplete remains and spurious comparisons with other similar-sized theropods.

Here we describe a nearly complete, partially articulated tail of a subadult individual of *Spinosaurus aegyptiacus (*FSAC-KK 11888), from the Cretaceous Kem Kem beds of south-eastern Morocco (Figs. 1, 2, Extended Data Figs. 1-4, Supplementary Information Part 1, Supplemental Information Video 1). The skeleton represents the most complete dinosaur known from the Kem Kem[21,22] and the most complete skeleton of a Cretaceous theropod from mainland Africa (Supplemental Information Part 2). As we show here, the tail forms part of the neotype of *S. aegyptiacus*[7] and was found in direct juxtaposition to the remainder of the skeleton (Extended Data Fig. 3). Over 90% of the new material, which confirms that a single subadult individual is preserved at the site, was recovered during field excavations in late 2018 and digitally recorded (Extended Data Fig. 5, Supplementary Information Parts 2-4). Several elements compare closely to drawings of *Spinosaurus* fossils destroyed in World War II (Extended Data Fig. 6).

More than 30 near-sequential caudal vertebrae (located within caudal positions 1-41) of FSAC-KK 11888 are preserved, representing approximately 80% of original tail length (Extended Data Figs. 3, 4, Extended Data Table 1). Both proximal and distal elements of the tail are complete and preserved in three-dimensions, indicating minimal taphonomic distortion (Fig. 2, Supplemental Information Video 2). At the level of the caudal transition point[1], the centra become proportionally more elongate. In addition, the prezygapophyses no longer overhang the preceding centrum and show a marked decrease in size compared to many theropod dinosaurs[1]. The postzygapophyses also decrease in size, leading to a reduced contact with the prezygapophyses, and are completely absent in the distalmost caudal vertebrae (Fig. 2). This again is different from the condition seen in most theropods, where zygapophyses become more elongate and more prominent toward the tail tip[1] restricting flexibility in more distal intervertebral joints.

The neural arches are distinctive elements of the *Spinosaurus* tail. A remarkable complex of vertebral laminae and fossae is present in the proximal caudal vertebrae, and partly persists in mid-caudal neural arches. The morphology of the neural spines shows considerable variation along the sequence (Figs. 1, 2, Extended Data Table 1): spines of proximal caudals are about three times taller than their centra and are cross-shaped in cross-section from base to mid-height, in mid-caudals the spines become much longer, and in the small distal caudals neural spine length reaches well over seven times the height of the centrum (contra ref.[11]). The neural spines of mid-distal caudal vertebrae of *Spinosaurus* have a unique cross-section, whereby they are proximo-distally rather than mediolaterally flattened. This is due to hyper-developed spinodiapophyseal laminae and loss of pre- and postspinal laminae. The tail chevrons also differ from those of other theropods. Their morphology varies little throughout the caudal series, except for a slight gradual reduction of the haemal canal: distal chevrons are as elongate as the proximal ones, but they become slender, paralleling the gradual decrease in size of the centra. Taken together, the elongated neural and haemal arches result in a dramatic, vertically expanded tail shape with extensive lateral surface area (Supplemental Information Fig. 4).

The skeletal anatomy of *Spinosaurus* represents a major departure from that of other theropods including the clade within which it is located[1], the basal Tetanurae, which comprises crown group birds and all other stem theropods more closely related to birds than to *Ceratosaurus*[1]. A key feature of this group is a stiffened tail in which the degree of overlap in articulation between pre- and postzygapophyses increases along the caudal series, drastically diminishing the range of motion between individual vertebrae[1]. This trend in motion reduction is emphasised in paravians with the appearance of ossified ligaments and/or reduction and fusion of the caudals into a pygostyle[17]. By contrast, in *Spinosaurus* the pre- and postzygapophyses are much further reduced

than in other tetanurans and, in the mid and distal portion of the tail, not only do not overlap but almost disappear, allowing the caudal region considerable flexibility, especially with regard to lateral movements (Fig. 2).

The highly-specialized tail morphology in *Spinosaurus* is thus hypothesized to have functioned as a propulsive structure for aquatic locomotion. To test this idea, we evaluated the swimming potential of the *Spinosaurus* tail shape by comparing it to the tails of two terrestrial theropods (*Coelophysis bauri* and *Allosaurus fragilis*), two semi-aquatic tetrapods (the crocodile *Crocodylus niloticus* and the crested newt *Triturus dobrogicus*), and a rectangular control. Two-dimensional tail shapes were cut from 0.93 mm thick plastic of flexural stiffness $5.8 * 10^{-5}$ Nm^2. The plastic tails were attached to a robotic controller and actuated in a water flume to provide tail tip amplitudes approximately 40% of tail length during swimming at 0.5 tail lengths/second. This swimming speed and amplitude of motion is similar to that of slow aquatic locomotion in modern tetrapods[23,24,25]. Measurement of swimming performance was assessed by quantifying mean thrust and efficiency using a six-axis force-torque sensor attached to the shaft driving each tail shape[26] (Fig. 3, Methods, Supplementary Information Fig. 4, Supplementary Information Videos 3-5).

Our experimental results show that the *Spinosaurus* tail shape was capable of generating more than eight times the thrust of the other theropod tail shapes and achieved 2.6 times the efficiency (Fig. 3). The greatest thrust was achieved by the crested newt tail shape (1.8 times *Spinosaurus*; 14.8 times *Coelophysis*), but the crocodile tail shape achieved greater propulsive efficiency (1.5 times *Spinosaurus;* 4.0 times *Coelophysis*), comparable to the rectangular control (Fig. 3). The lower efficiency recovered in this experiment for *Spinosaurus* (compared to the control) and the crested newt indicates an effect of tail shape on performance. Overall, the vertically expanded tail shape of *Spinosaurus* imparts a substantial positive benefit to aquatic propulsion relative to the long and

narrow tails of terrestrial theropods, supporting the inference that *Spinosaurus* utilized tail propelled swimming. This tail morphology may have also increased lateral stability of the body in the water, reducing the tendency to roll while floating[10].

Contrary to recent suggestions[10] that *Spinosaurus* was confined to wading and the apprehension of prey from around the edges of water bodies, the morphology and function of the tail along with other adaptations for life in water[7] point to an active, highly specialized aquatic predator that pursued and caught its prey in the water column (Extended Data Fig. 7). The skeletal remains of *Spinosaurus* (SI) from the Kem Kem beds – composed of sediments deposited in a major fluvio-deltaic system[7] that have yielded a diverse vertebrate assemblage[27] – provide further insights into the ecology of this dinosaur. The Kem Kem assemblage is highly atypical, containing a rich freshwater fauna dominated by fish, including lungfish and large to very large sawfish, and coelacanths[27], a diverse range of crocodyliforms[28], and several giant predatory dinosaurs[7,22]. The seemingly anomalous occurrence in the same deposits of several large-bodied predators, but few terrestrial herbivores, is partially explained by the fully aquatic, likely piscivorous, lifestyle of *Spinosaurus* which considerably expands the morphological and ecological disparity of Kem Kem tetrapods[7, 29]. At the same time, competition with several co-occurring large aquatic predators[28] may have driven the evolution of giant size in *Spinosaurus*.

The discovery that an evolutionarily significant clade of dinosaurs exploited environments previously thought to be uninhabited by this group highlights weaknesses in current datasets upon which global evolutionary narratives are based. Dinosaur anatomy and functional morphology are perhaps rather less well understood than often claimed[30]. This is likely related, in part, to the under-representation of dinosaur remains from Africa, the sampling of which lags far behind that of Europe, Asia and North America[1]. Other African dinosaurs preserved in similar settings, such as

the poorly understood “hippopotamus ornithopod” *Lurdusaurus*[31], may also have been better adapted to aquatic settings than currently recognized, further emphasising current limitations to our comprehension of these animals.

References

1. Weishampel D. B., Dodson P., & Osmólska H. *The Dinosauria* 2nd edn. (Berkeley, Univ. of California Press, 2004).
2. Owen, R. A description of a portion of the skeleton of the *Cetiosaurus*, a gigantic extinct saurian reptile occurring in the oolitic formations of different portions of England. *Proceedings of the Geological Society of London* **3**, 457-462 (1841).
3. Cope, E. On the characters of the skull in the Hadrosauridae. *Proceedings of the National Academy of Sciences of Philadelphia* **35**, 97-107 (1883).
4. Kermack, K. A. A note on the habits of sauropods. *Annals and Magazine of Natural History* **12**, 830-832 (1951).
5. Bakker, R. T. Ecology of the brontosaurs. *Nature* **229,** 172-174 (1971).
6. Alexander, R. McN. Mechanics of posture and gait of some large dinosaurs. *Zool. J. Linn. Soc.*, **83**, 1–25 (1985).
7. Ibrahim, N. *et al*. Semiaquatic adaptation in a giant predatory dinosaur. *Science* **345**, 1613-1616 (2014).
8. Aureliano, T. *et al*. Semi-aquatic adaptations in a spinosaur from the Lower Cretaceous of Brazil. *Cretaceous Res.* **90**, 283-285 (2018).

9. Evers, S. W., Rauhut, O. W., Milner, A. C., McFeeters, B. & Allain, R. A reappraisal of the morphology and systematic position of the theropod dinosaur *Sigilmassasaurus* from the "middle" Cretaceous of Morocco. *PeerJ* **3**, e1323 (2015).

10. Henderson, D. M. A buoyancy, balance and stability challenge to the hypothesis of a semi-aquatic *Spinosaurus* Stromer, 1915 (Dinosauria: Theropoda). *PeerJ* **6**, e5409 (2018).

11. Hone, D. W. E. & Holtz, T. R. Comment on: Aquatic adaptation in the skull of carnivorous dinosaurs (Theropoda: Spinosauridae) and the evolution of aquatic habits in spinosaurids. *Cretaceus Res.* **93**, 275-284 (2019).

12. Stromer, E. Ergebnisse der Forschungsreisen Prof. E. Stromers in den Wüsten Ägyptens. II. Wirbeltier-Reste der Bahariye-Stufe (unterstes Cenoman). 3. Das Original des Theropoden *Spinosaurus aegyptiacus* nov. gen., nov. spec. *Abh. Kgl. Bayer. Akad. Wiss. Math. Phys. Kl. München* **28,** 1-28 (1915).

13. Vullo, R. *et al*. Convergent Evolution of Jaws between Spinosaurid Dinosaurs and Pike Conger Eels. *Acta Paleontol. Pol.* **61**, 825-829 (2016).

14. Arden, T. M. S., Klein, C. G., Zouhri, S. & Longrich, N. R. Aquatic adaptation in the skull of carnivorous dinosaurs (Theropoda: Spinosauridae) and the evolution of aquatic habits in *Spinosaurus*. *Cretaceous Res.* **93**, 275-284. (2019).

15. Charig, A. J. & Milner, A. C. *Baryonyx walkeri*, a fish-eating dinosaur from the Wealden of Surrey. *Bull. Nat. Hist. Mus. Geol.* **53**, 11-70 (1997).

16. Sues, H. D., Frey, E., Martill, D. M. & Scott, D. M. *Irritator challengeri*, a spinosaurid (Dinosauria: Theropoda) from the Lower Cretaceous of Brazil. *J. Vert. Pal.* **22**, 535-347. (2002).

17. Witmer, L. M. The debate on avian ancestry: Phylogeny, function, and fossils. in *Mesozoic Birds: Above the Heads of Dinosaurs* (eds. Chiappe, L. M. & Witmer, L. M.) 3–30 (Univ. California Press, 2002).

18. Tereshchenko, V. Adaptive features of protoceratopoids (Ornithischia, Neoceratopsia). *Paleontol. Journal* **42**, 273-286 (2008).

19. Cau, A. *et al*. Synchrotron scanning reveals amphibious ecomorphology in a new clade of bird-like dinosaurs. *Nature* **552**, 395–399 (2017).

20. Sereno, P. C. *et al*. A long-snouted predatory dinosaur from Africa and the evolution of spinosaurids. *Science* **282**, 1298-1302 (1998).

21. Lavocat, R., Comptes rendus 19e Congrés géologique international (Alg.) 1952. *Acad. Sci. Paris* **15**, 65 (1954).

22. Sereno, P. C., Dutheil, D. B., Iarochene, M. & Larsson, H. C. Predatory dinosaur from the Sahara and Late Cretaceous faunal differentiation. *Science* **272**, 986-991 (1996).

23. D'Août, K. & Aerts, P. Kinematic and swimming efficiency of steady swimming in adult axolotls (*Ambystoma mexicanum*). *J. Exp. Biol.* **200**, 1863-1871 (1997).

24. Fish, F. Kinematics of undulatory swimming in the American alligator. *Copeia* **4***,* 839-843 (1984).

25. Frolich, L. M. & Biewener, A. A. Kinematic and electromyographic analisys of the functional role of the body axis during terrestrial and aquatic locomotion in the salamander *Ambystoma tigrinum*. *J. Exp. Biol.* **162**, 107-130 (1992).

26. Lauder G. V., Flammang B. E. & Alben S. Passive robotic models of propulsion by the bodies and caudal fins of fish. *Integr. Comp. Biol.* **52**, 576–587 (2012).

27. Cavin, L. *et al*. Vertebrate assemblages from the early Late Cretaceous of southeastern Morocco: an overview. *J. Afr. Earth Sci.* **57**, 391-412 (2010).

28. Meunier, L. M. V. & Larsson, H. C. E. Revision and phylogenetic affinities of *Elosuchus* (Crocodyliformes). *Zool. J. Linnean Soc.* **179**, 169-200 (2017).

29. Amiot, R. et al. Oxygen and carbon isotope compositions of middle Cretaceous vertebrates from North Africa and Brazil: ecological and environmental significance. Paleogeogr. Paleoclimatol Paleoecol. ***297****, 439-451 (2010).*

30. *Brusatte, S. L. Dinosaur Paleobiology (John Wiley & Sons, 2012).*

31. Taquet, P. The African cousins of the European iguanodontids. in *Bernissart dinosaurs and Early Cretaceous terrestrial ecosystems* (ed. Godefroit, P.) 283–291 (Indiana University Press, 2012).

Supplementary Information is available in the online version of the paper.

Acknowledgements

We thank Mhamed Azroal, Hamid Azroal, and M'Barek Fouadassi for assistance in the field. Ammar Aït Ha is thanked for help in preparing the fossils. The Moroccan Ministry of Mines, Energy and Sustainable Development is thanked for providing fieldwork permits. We thank Fabio Manucci for helpful discussions about the flesh reconstruction of *Spinosaurus*. This research was supported by a National Geographic Society grant to NI [CP-143R-17], a National Geographic Emerging Explorer Grant to NI, contributions from the Board of Advisors of the University of Detroit Mercy to NI, a Jurassic Foundation grant to MF, a Paleontological Society grant to MF, an Explorers club grant to MF, as well as financial support from the Lokschuppen Rosenheim, the Museo di Storia Naturale di Milano, Joachim Pfauntsch, and Alessandro Lania.

Author Contributions

N.I. led the expeditions and the project. N.I., S.M., C.D.S., M.F., M.A., D.M.M., G.B., S.Z. D.M. and A.A. collected the specimens in the field. N.I., S.M., C.D.S., M.F., J.W., G.V.L. and S.E.P. designed the research. N.I., S.M., C.D.S., M.F., J.W., G.V.L. and S.E.P. designed and performed the experiments. N.I., S.M., C.D.S., M.F., M.A., D.M.M., J.W., G.B., S.Z. D.M., D.M.U., U.J., J.J., A.A., G.V.L., S.E.P. analyzed the data. G.B., M.A., C.D.S., S.E.P., D.M.M., S.M., and D.B. created the figures. D.B. sculpted the scientific reconstruction. N.I., S.M., C.D.S., M.F., J.W., D.M.U, G.V.L., S.E.P. wrote the manuscript which was reviewed by all authors.

Conflicts of Interest Declaration

The authors declare no financial or non-financial competing interests. Correspondence and requests for materials should be addressed to N.I. (ibrahini@udmercy.edu).

Data Availability Statement

The authors declare that all data supporting the findings of this study are available within the paper and its Supplementary Information and Source data.

Figures

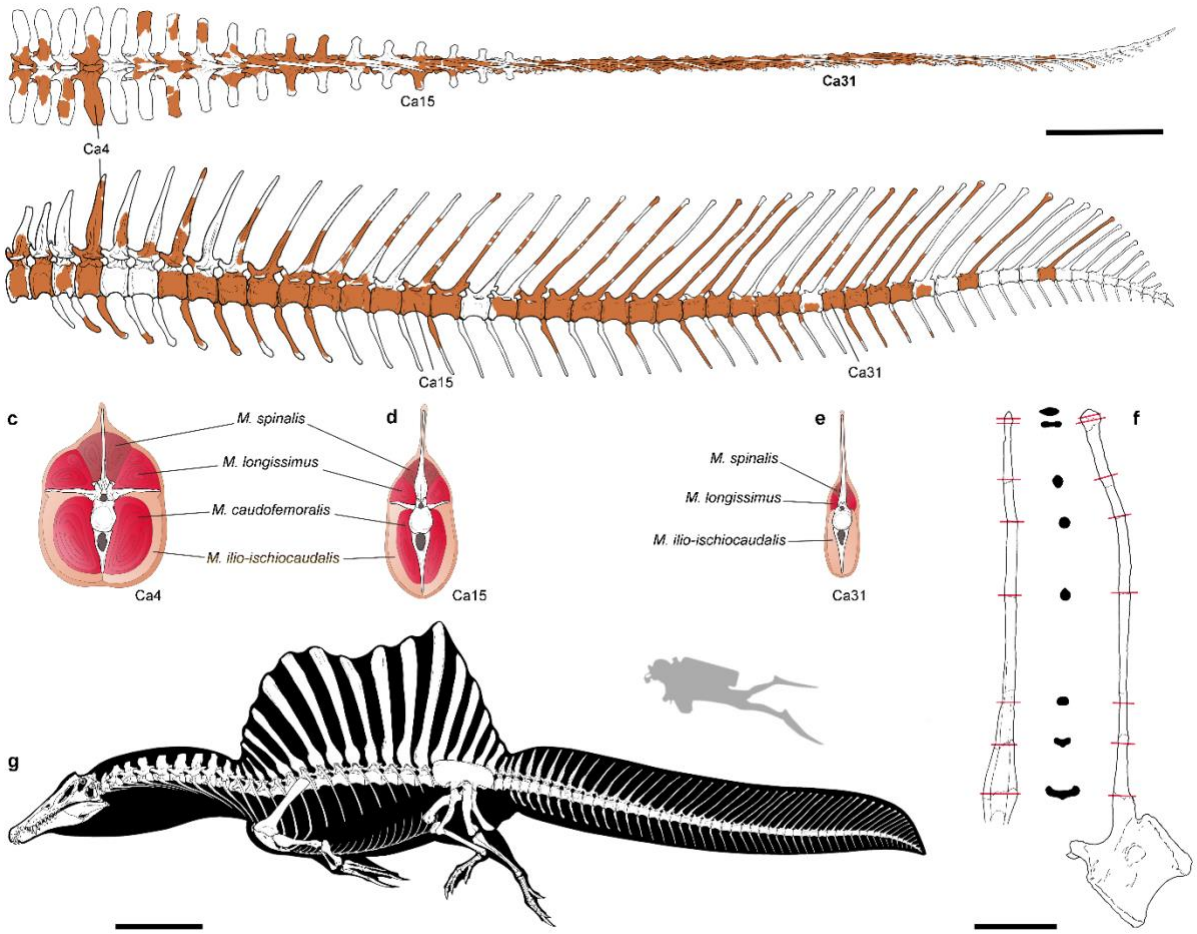

Figure 1 Reconstructed skeleton and caudal series of *Spinosaurus* FSAC-KK 11888. Caudal series (preserved parts in colour) in **a,** dorsal view; **b**, left lateral view; **c-e**, reconstructed sequential cross sections through the tail show proximal/distal changes in the arrangement of major muscles; **f**, sequential cross sections (proximal face pointing upwards) through the neural spine of vertebra Ca23 to show apicobasal changes (see text). **g**, skeletal reconstruction. Abbreviations: Ca: caudal vertebra. Scale bar = 50 cm (a-e), 10 cm (f), 1m (g).

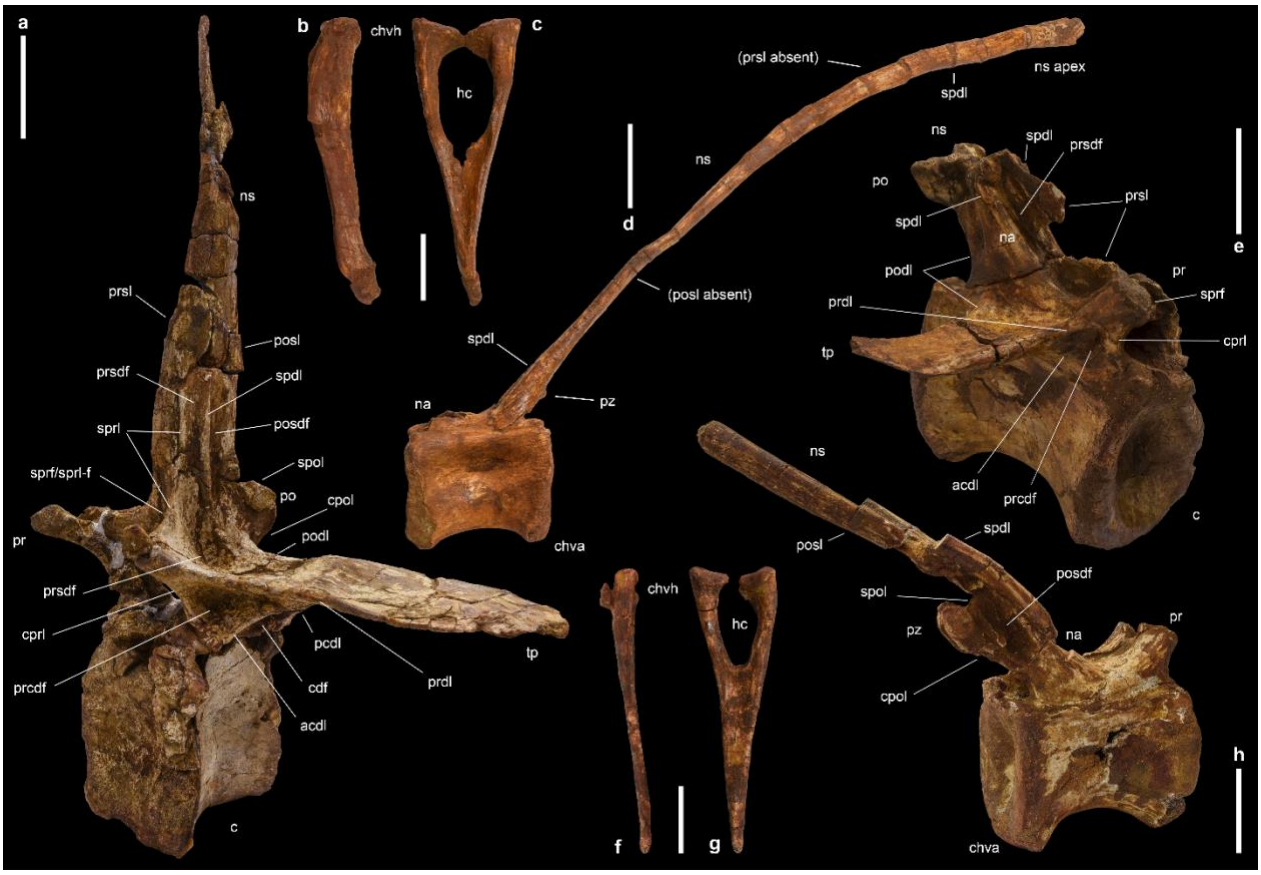

Figure 2 Selected caudal vertebrae and chevrons of *Spinosaurus aegyptiacus* FSAC-KK 11888. a, proximal caudal (Ca4) in left proximolateral view. **b-c**, proximal chevron (Chv7) in left lateral and proximal view. **d**, distal caudal (Ca31) in left lateral view. **e**, mid-caudal (Ca12) in right proximolateral view. **f-g**, distal chevron (Chv27) in left lateral and proximal view. **h**, mid-caudal (Ca16) in right lateral view. Abbreviations: acdl, anterior centrodiapophyseal lamina; c, centrum; ca, caudal vertebra; cdf, centrodiapophyseal fossa; chva, chevron articulation; chvh, chevron head; cpol, centropostzygapophyseal lamina; cprl, centroprezygapophyseal lamina; hc, haemal canal; ns, neural spine; pcdl, posterior centrodiapophyseal lamina; po, postzygapophysis; pocdf, postzygapophyseal centrodiapophyseal fossa; podl,

postzygodiapophyseal lamina; posdf, postzygapophyseal spinodiapophyseal fossa; posl, postspinal lamina; pr, prezygapophysis; prcdf, prezygapophyseal centrodiapophyseal fossa; prdl, prezygodiapophyseal lamina; prsdf, prezygapophyseal spinodiapophyseal fossa; prsl, prespinal lamina; na, neural arch; ns, neural spine; spdl, spinodiapophyseal lamina; spol, spinopostzygapophyseal lamina; spof, spinopostzygapophyseal fossa; sprl, spinoprezygapophyseal lamina; sprl-f, spinoprezygapophyseal lamina fossa; tp, transverse process. Scale bars = 10 cm in a, 5 cm in b-h.

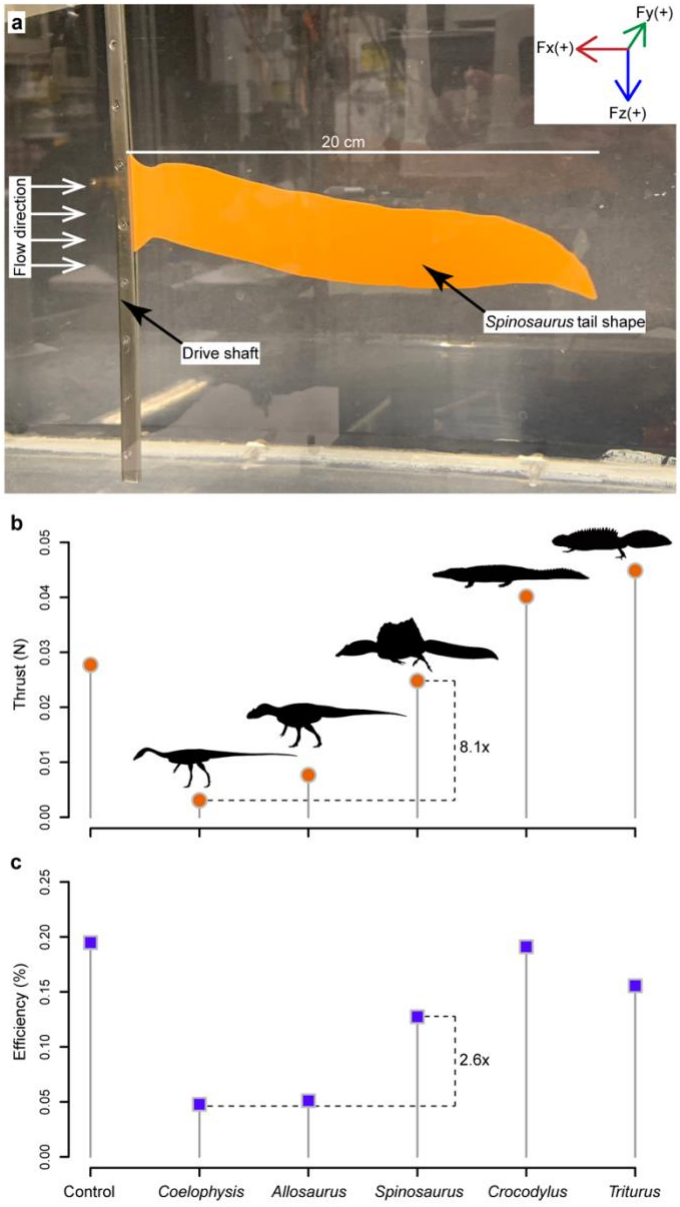

Fig. 3: **Thrust and efficiency of six different tail shapes during swimming. a,** The *Spinosaurus* plastic tail shape attached to the robotic driving shaft in the water flume. The water is flowing from left to right at 10 cm/s. The coordinate system is provided in the top right. With reference to the tail, positive x forces (Fx) are generated anterior (or upstream), positive y forces (Fy) in the right lateral direction, and positive x forces (Fz)

in the ventral direction. **b,** Mean thrust and **c,** mean efficiency generated by tail shapes during robotically-controlled swimming. All tails were scaled to the same total length of 20 cm (Supplementary Information Fig. 4). The control tail was cut as a rectangular shape with the same surface area as the scaled *Spinosaurus* tail (63 cm^2). Details of the experimental setup are given in the methods. Raw thrust and efficiency data for each tail, including mean and standard error, are provided in Supplementary Data Table 2. Swimming motions of the *Spinosaurus* tail can be found in Supplementary Videos 3-5.

Methods

Excavation

The Cretaceous Kem Kem beds of Morocco crop out along an extensive escarpment near the Moroccan-Algerian border region[7]. After the accidental discovery and partial excavation by a local collector in 2008, part of a single skeleton (FSAC-KK 11888), subsequently deposited at the Faculté des Sciences of Casablanca University (FSAC), was recovered, published and designated as the neotype[7]. A multi-institutional collaborative project in the years 2015-2019, led by NI, resulted in four joint expeditions to the neotype site. Detailed and careful exploration of the debris around the site, as well as a systematic and complex excavation of the unexcavated portion of the fossiliferous layer of the Zrigat hill, led to the recovery of many additional elements of the neotype skeleton (Extended Data Figure 1, Extended Data Figure 2). A detailed description of the new material, as well as the geological context, is included in the Supplemental Information. The supplemental information also includes details on a full-body flesh reconstruction based on FSAC-KK 11888.

Experimental testing of tail shape swimming performance.

To test the aquatic locomotor potential of the newly reconstructed *Spinosaurus aegyptiacus* tail, we determined the swimming performance of its tail shape using a robotic controller developed for studies of propulsive hydrodynamics[31,32,33,34,35]. The swimming performance of the S*pinosaurus* tail shape was compared to the performance of five other tail shapes from the following species: the small-bodied terrestrial theropod *Coelophysis bauri*, the large-bodied terrestrial theropod *Allosaurus fragilis*, the semi-aquatic crocodile *Crocodylus niloticus*, the semi-aquatic crested newt *Triturus dobrogicus*, and a rectangular control tail that was scaled to the same surface area as the *Spinosaurus* tail. Tail shapes (Supplemental Information Fig. 4) were all scaled to 20 cm anteroposterior length (L), manufactured from 0.93 mm thick plastic of flexural stiffness $5.8 * 10^{-5}$ Nm^2 and cut using an Epilog Zing24 laser cutter.

The plastic tails were attached to a robotic controller that allowed us to impose specific motion programs on the rigid shaft to which each tail was affixed (Supplementary Information Fig. 5, Supplemental Information Videos 3-5). This shaft was moved in both heave (side-to-side) motion, as well as in pitch (angular rotation) to achieve undulatory tail motions. The imposed motion program was 1 Hz frequency, +/- 1 cm heave, and +/- 25° pitch which resulted in the tail tip undergoing peak-to-peak lateral excursions of approximately 40% L, comparable to that exhibited by swimming axolotl and alligators[23,24,25].

The shaft supporting each tail at the leading edge was attached to an ATI Inc. (Apex, NC, USA) Nano-17 six-axis force/torque sensor located just above the water surface. Testing occurred in a recirculating water flume and a free-stream flow of 0.5 L (10 cm/s) was imposed for all tests. Custom LabVIEW programs (National Instruments Corp., Austin, TX, USA) were used to control flapping frequency, flow speed, foil heave, and pitch. A custom LabVIEW program also was used to acquire data from the ATI transducer at a sampling rate of 1000 hz. Each tail shape

was tested N=5 times, except for the *Spinosaurus* tail which was tested N=5 times on two different days for a total of N=10 tests. Output data can be found in Supplementary Information Table 1.

Thrust and efficiency for each tail shape were calculated using standard fluid dynamic equations as in our previous research[36,37]. Mean thrust force (Fx) is calculated directly from transducer output from the Fx channel, and we accounted for transducer rotation resulting from the pitch motion to provide the force component directed upstream (positive thrust). Propulsive efficiency is calculated as the ratio of the thrust coefficient ($C_T = 2\overline{F}x/\rho U^2 cs$) to the power coefficient ($Cp = 2\overline{P}/\rho U^3 cs$) where ρ is the fluid density, U swimming velocity, c foil chord, and s the tail span. Effectively, this metric assesses the extent to which input power is translated into thrust.

Osteohistological analysis.

The aim of the osteohistological analysis was to determine if the remains assigned to FSAC-KK 11888 belong to a single individual rather than a chimaeric association of juvenile and adult individuals preserved in the same location and at the same horizon. The analysis was based on five selected elements. The primary assumption is that should histological details suggest that all five elements represent the same ontogenetic stage then they are more likely to represent one rather than multiple individuals. By contrast, should these elements exhibit two, or more, distinct ontogenetic stages this would point to the presence of multiple individuals of one, or perhaps several, taxa, all fortuitously preserved at a single location during a single depositional event[38, 39, 40].

The following elements were sectioned: the right femur; the left fibula; one rib; and two neural spines. All specimens were sectioned prior to preparation, in order to ensure that no outer layers

of the compact cortex were accidentally removed. In the case of the neural spines the apical portion was sectioned.

Thin sectioning followed standard protocol[41]. The thin sections have a thickness of 50-70 microns and were analyzed with a petrographic microscope, Leica DM 2500 P. Digital images were captured using a ProgRes Cfscan camera. Only continuous lines were counted as lines of arrested growth (LAGs). Annuli were interpreted as a single year, following Lee and O'Connor[42]. Retrocalculation, following the method proposed by Horner & Padian[43], was applied to determine the likely number of missing LAGs, eroded through remodelling of the bone. In the case of the neural spines, only the width of the inner-most zone was used to retrocalculate the missing LAGs, because the shape of the section could not be approximated to a circular outline. The calculation of the major and minor axis used for the retrocalculation was performed in ImageJ[44]. Results of the histological analysis are included in Supplemental Information.

32. Lauder G. V., Anderson E. J., Tangorra J. & Madden P. G. A. Fish biorobotics: kinematics and hydrodynamics of self-propulsion. *Journal of Experimental Biology* **210**, 2767-2780 (2007).

33. Lauder G. V. *et al*. Robotic models for studying undulatory locomotion in fishes. *Marine Technology Society Journal* **45**, 41-55 (2011).

34. Quinn, D. B., Lauder, G. V. & Smits, A. J. Maximizing the efficiency of a flexible propulsor using experimental optimization. *Journal of Fluid Mechanics* **767**, 430-448 (2015).

35. Rosic M. L., Thornycroft P. J. M., Feilich K., Lucas K. N. & Lauder G. V. Performance variation due to stiffness in a tuna-inspired flexible foil model. *Bioinspiration & Biomimetics* **12**, 016011. (2017).

36. Saadat M. *et al*. On the rules for aquatic locomotion. *Physical Review Fluids* **2**, 083102 (2017).

37. Read, D. A., Hover, F. S. & Triantafyllou, M. S. Forces on oscillating foils for propulsion and maneuvering. *J. Fluids Struct.* **17**, 163-183 (2003).

38. Shelton, M. R., Thornycroft, P. & Lauder, G. Undolatory locomotion of flexible foils as biomimetic models for understanding fish propulsion. *The Journal of Experimental Biology* **217**, 2110-2120 (2014).

39. Ryan, M. J., Russell, A. P., Eberth, D. A. & Currie, P. J. The taphonomy of a *Centrosaurus* (Ornithischia: Certopsidae) bone bed from the Dinosaur Park Formation (Upper Campanian), Alberta, Canada, with comments on cranial ontogeny. *Palaios* **16**, 482-506 (2001).

40. Erickson, G. M., Currie, P. J., Inouye, B. D. & Winn, A. A. Tyrannosaur life tables: an example of nonavian dinosaur population biology. *Science* **313**, 213-217 (2006).

41. Bertozzo, F., Dalla Vecchia, F. M. & Fabbri, M. The Venice specimen of *Ouranosaurus nigeriensis* (Dinosauria, Ornithopoda). *PeerJ* **5**, e3403 (2017).

42. Chinsamy, A. & Raath, M. A. Preparation of fossil bone for histological examination. *Palaeontol. Afr.* **29**, 39-44 (1992).

43. Lee, A. H. & O'Connor, P. M. Bone histology confirms determinate growth and small body size in the noasaurid theropod *Masiakasaurus knopfleri*. *Journal of Vertebrate Paleontology* **33**, 865-876 (2013).

44. Horner, J. R. & Padian, K. Age and growth dynamics of *Tyrannosaurus rex*. *Proceedings of the Royal Society of London B: Biological Sciences* **271**, 1875-1880 (2004).

45. Schneider, C. A., Rasband, W. S. & Eliceiri, K. W. NIH Image to ImageJ: 25 years of image analysis. *Nature methods* **9**, 671-675 (2012).

Extended data figures and tables

Extended data Figure 1 | Excavation of the *Spinosaurus* (FSAC-KK 11888) site. (a-f) Different stages of the excavation, which resulted in the removal of over 15 tons of rock using a range of tools, including picks, brushes, hammers, and a jackhammer. a) November 17th, 2013; b) March 29th, 2015; c) September 17th, 2018; d) September 19th, 2018; e) December 5th, 2018; f) July 21st, 2019. (g-h) Selected bones in situ. g) Largely complete proximal caudal (Ca4) vertebra; h) Neural spine of a mid-distal caudal vertebra, fragmented by syndiagenetic cracks. Scale bars = 10cm.

Extended Data Figure 2 | Excavation of caudal elements of *Spinosaurus* (FSAC-KK 11888). (a) Largely complete distal caudal vertebra (Ca31), recovered in its entirety by digging a tunnel until the apex of the neural spine was reached; (b) semi-articulated mid-caudal vertebrae, (c) two haemal arches, (d) close association of middle caudal elements. Scale bars = 10 cm.

Extended Data Figure 3 | Excavation map and skeletal reconstruction. Detailed map of the site of discovery of the *Spinosaurus aegyptiacus* neotype (FSAC-KK 11888), and fully revised skeletal reconstruction. The map and reconstruction's colors correspond to different phases of excavation: the local discovery in 2007-2008 (**red**), our excavations during the 2015-2019 expeditions (**green**), and sieving in the debris area during the 2015-2019 expeditions (**yellow**). Both images are at the same scale. Scale bar 1 m.

Extended Data Figure 4 | The caudal series of *Spinosaurus aegyptiacus* (FSAC-KK 11888). Photograph of entire caudal series (numbered). Scale bar = 1 m.

Extended Data Figure 5 | Elements of FSAC-KK 11888 from 2008 (first excavation) and 2019 (most recent), matched. Evidence of perfect match between elements collected by the local discoverer of the site (2007-2008**: a**, **e, f, i, k, m, n, p, q, s**) and elements excavated *in situ* or recovered from the site debris by Ibrahim et al. (2015-2019: **b**, **c**, **d, g, h, j, l, o, r, t**). **a-b**, right and left metatatarsal II. **c**, left penultimate phalanx of the fourth pedal digit (IV-4) that came to light within the typical matrix in which bones of the *Spinosaurus* neotype (FSAC-KK 11888) were embedded. **d-e**, two ?splenial fragments reconnected. **f-i**, phalanx IV-4 prepared and compared to the counter-lateral element of the right pes in dorsal view, and rearticulated with its ungual. **j-m**, two complementary (broken) halves of the left squamosal and of a dorsal rib. **n-p** and **s-t**, two key-fragments from the debris, reconnecting the base and the shaft of the ?7th neural spine. **q-r**, the right astragalus (excavated *in situ* in July 2019) rearticulated to its tibia (from 2008). Arrows point to recomposed fractures.

Extended Data Figure 6 | Comparison of neotype caudals (FSAC-KK 11888) to those destroyed in WWII. Comparison between the caudal vertebrae of the neotype of *S. aegyptiacus*, with those of the two, now lost, specimens described by Stromer. Proximal caudal vertebra of the

holotype (BSP 1912 VIII 19) in distal (**a**) and right lateral (**c**) views; Ca 4 of the neotype in distal (**b**) and right lateral (**d**) views. Anterior caudal vertebra of *Spinosaurus* B in dorsal (**e**), right lateral (**g**), and proximal (**i**) views; Ca 11 of the neotype in dorsal (**f**), right lateral (**h**), and proximal (**j**) views. Middle caudal vertebra of *Spinosaurus* B in dorsal (**k**), left lateral (**m**) and distal (**o**) views; Ca 21 of the neotype (FSAC-KK 11888) in dorsal (**l**), left lateral (**n**) and distal (**p**) views. Scale bars =10 cm.

Extended Data Figure 7 | 3D fleshed out model based on FSAC-KK 11888. Symmetrical pose in five views (**a**) and swimming pose (**b**).

Extended Data Table 1 | Measurements of caudal vertebrae of FSAC-KK 11888. Measurements are in mm; (p) = not complete, measured as preserved; n.p. = not preserved; n.a., not applicable; e, estimated.

Extended Data Table 2 | Measurements of chevrons of FSAC-KK 11888. Measurements are in mm; (p) = not complete, measured as preserved; n.p. = not preserved; e, estimated.